Abrasion resistance of thermal sprayed composite coatings with a nickel alloy matrix and a WC hard phase. Effect of deposition technique and re-melting

J.C. Miranda [a] and A. Ramalho [b]

[a] *Esc. Sup. de Tecnologia e Gestão, Inst. Politec. da Guarda, 6300 Guarda, Portugal*
[b] *Dep. Eng. Mec., Univ. Coimbra, Pólo II, Pinhal de Marrocos, 3030 Coimbra, Portugal*

Received 9 October 2000; accepted 23 February 2001

Coatings resulting from the spraying of mixtures with different proportions of two commercial alloys, a nickel self-fluxing alloy and a tungsten carbide with cobalt, have been produced using two flame-spraying techniques: HVOF, and powder oxy-acetylene flame spraying. The effect of both hard-phase content and coating-spraying technique on abrasion resistance is discussed in terms of the coatings' mechanical properties and microstructure.

KEY WORDS: abrasion resistance; thermal spray; coatings

1. Introduction

Thick coating deposition by means of different thermal-spraying systems has been shown to be a suitable procedure for obtaining and restoring engineering components with high-performance properties, operating with high surface requirements, namely tribological or oxidation/corrosion. The performance required of surface components leads to the use of materials with high levels of hardness, toughness and also resistance to wear and oxidation. Achieving all these properties in the bulk materials normally used is difficult, but the development of surface engineering has made it possible to balance and adapt them to the demands of each application. Recourse is made to materials composed of metal alloys and metal and ceramic mixtures, forming specially developed composite systems and aiming at predetermined mechanical and physical–chemical properties. Thermal-sprayed coatings improve component performance relative to the bulk material used as substrate. The application of coatings to improve wear resistance employs materials that include elements which form hard and stable carbides, such as titanium, molybdenum and tungsten. Applying tungsten carbide in a cobalt alloy matrix is an example where it is possible both to optimise the hardness through the increase of volumetric fraction of carbide and to maximise toughness by increasing the volumetric fraction corresponding to the ductile matrix. The popularity of thermal spraying systems is mainly due to the fact that it can change, almost independently, the fraction corresponding to each of the phases, easily modifying microstructure and granulometry.

Nowadays, there are several spraying processes that make it easy to achieve high-quality thick coatings. These techniques are characterised by different conditions of temperature and spraying kinetics, leading to the production of coatings with a wide range of properties.

For applications that require abrasion and sliding resistance at operating temperatures of up to 500 °C, tungsten carbide cermets, with cobalt as binder, is widely selected from the available materials. For this kind of material, the best performance properties are obtained when the WC phase has a higher level than the W_2C and W_3Co_3C phases (or other carbide mixes, such as M_6C). The spraying technique has an important influence on the presence of phases of lower hardness and wear resistance, as well as on the oxidation level of the sprayed material [1].

For applications requiring a matrix with high tenacity and oxidation resistance, many coating producers offer thermal sprayed coatings based on nickel alloys. Wang et al. [2] have found that nickel-based coatings with a WC hard phase perform well in combustion engines that have to work in abrasive environments, such as desert regions. However, the relative effect of each phase on the coating's properties has not yet been demonstrated for this kind of coating. Although it is known that the coating re-melt produces a WC phase decomposition, it remains to be determined if this damaging effect is counterbalanced by the fact that thinner structures are obtained through WC + Co grain desegregation resulting from the melting of the binder. Thus, the purpose of this work is to compare the mechanical properties of WC coatings in a metallic matrix, using two different spraying techniques: HVOF spraying (high-velocity oxy-fuel) and PFS (powder flame spraying). It aims to ascertain the influence of the spraying technique when the hard WC + Co phase comprises from 30 to 70 wt% of the total. It also seeks to verify the change in film characteristics when it is remelted after spraying. For this, steel substrates have been used, and the coating characteristics were compared in terms of mi-

crostructure, hardness, adhesion, porosity and abrasion resistance.

The PFS process is basically the spraying of molten material onto a surface to provide a coating. Material in powder form is melted in a flame (oxy-acetylene or hydrogen) to form a fine spray. When the spray contacts the prepared surface of a substrate material, the fine molten droplets rapidly solidify forming a coating. This process carried out correctly is called a "cold process" (relative to the substrate material being coated) as the substrate temperature can be kept low during processing, in order to avoid damage, metallurgical changes and distortion to the substrate material. The HVOF (high-velocity oxy-fuel) thermal spray process is basically the same as the PFS except that this process has been developed to produce an extremely high spray velocity. There are a number of HVOF guns which use different methods to achieve high-velocity spraying. One method basically consists of a high-pressure, water-cooled combustion chamber and a long nozzle. Fuel (kerosene, acetylene, propylene and hydrogen) and oxygen are fed into the chamber, and combustion produces a hot, high-pressure flame, which is forced down a nozzle, increasing its velocity.

So, the main difference between the two studied spraying techniques is the particle velocity. In the PFS process the particle velocity can range from 30 to 250 m/s while the HVOF technique leads to values above 400 m/s.

2. Experimental details

2.1. Techniques and deposition parameters

Two production techniques of flame spraying for coatings were selected, with significant differences with regard to their operating principle, cost and availability: the HVOF technique and PFS. The deposition parameters for each technique are summarised in table 1.

2.2. Materials

The coatings studied result from the spraying of mixtures with different proportions of two commercial alloys, namely a nickel self-fluxing alloy (alloy 1) and tungsten carbide with cobalt (alloy 2). Table 2 shows the chemical composition and table 3 gives the different combinations of the alloys.

A widely-used construction steel, DIN Ck45, was chosen as the substrate.

For the HVOF spraying technique, three kinds of coating were used, with varying percentages of WC + Co. Thus, one coating with 30% (wt%) WC + Co was produced, another with 50% (wt%) WC + Co and a third one with 70% (wt%) WC + Co.

In the PFS technique, besides the mixtures mentioned above, certain tendencies with respect to the result had to be confirmed. For this technique, in the abrasion study, mixtures with 40 and 60% (wt%) WC + Co were also tested. In this technique, besides the coatings as deposited, the role of remelting was also examined, in order to study what kind of improvements took place on the coatings relative to its

Table 1
Spray parameters.

	HVOF	Oxy-acetylene flame spraying
Equipment	Plasma Technick CDS-100	CastoDyn DS 8000
Gases	Oxygen 420 l/min Propylene 55 l/min	Oxygen 17 l/min Acetylene 16 l/min
Spray distance	300 mm	200 mm
Maximum temperature	2850 °C	3150 °C

Table 2
Chemical composition of the alloys.

	Chemical composition (wt%)								Particle
	C%	Si%	B%	Fe%	Cr%	Ni%	Co%	W%	(μm)
Alloy 1	0.75	4.3	3.1	3.7	14.8	Bal	–	–	20–53
Alloy 2	5.5	–	–	–	–	–	12.0	Bal	20–53

Table 3
Characterisation of the coatings.[a]

Process	Alloy 1 (NiBCFeSiCr) (%)	Alloy 2 (WC + Co) (%)	Re-melt	Adhesive strength (N/mm^2)	Porosity (%)	Results of X-ray diffraction		
						Ni	WC	W_2C
HVOF	70	30	No	48	0.5	xx	xx	x
	50	50	No	56	0.5	x	xx	x
	30	70	No	63	0.5	x	xx	x
Oxy-	70	30	No	31	4	xx	x	xx
acetylene	60	40	No	na	2	na	na	na
flame	50	50	No	35	2	xx	x	xx
spraying	40	60	No	na	2	na	na	na
	30	70	No	48	4	xx	x	xx
	70	30	Yes	29	0.5	xx	xx	x
	60	40	Yes	na	1	na	na	na
	50	50	Yes	48	2	xx	xx	x
	40	60	Yes	na	2	na	na	na
	30	70	Yes	51	4	xx	xx	x

[a] xx – main phase, X – traces detected, na – not available.

inherent properties such as adhesion, porosity, hardness and abrasion resistance.

In all cases, the coatings have an approximate thickness of 500 μm at the end of the process.

For the PFS coatings, a layer of alloy 1, approximately 5 μm thick, was first sprayed as an adhesion layer.

2.3. Coating characterisation

The coating microstructure was studied and analysed by examining the cross-section of fractured specimens with a Philips XL30 TMP scanning electron microscope. Coating hardness was evaluated by indentation testing using HMV-2000 Shimadzu equipment with a Vickers indenter, applying a load of 300 g for 15 s on the coated specimen cross-section. For each specimen, ten indentations were made to calculate the average value of micro-hardness. The X-ray diffraction method was used to analyse the coating structure. Standard charts (MIL STD-1687A(SH)) were used to determine the coatings' porosity. Pull tests were used to evaluate adhesion between the coating and the substrate, following the ASTM C 633-79 standard test method [3]. In the pull tests, three specimens were tested for each experimental condition. The coatings' abrasion resistance was determined through rubber wheel abrasion tests, using silica sand as an abrasive. The equipment layout is shown in figure 1.

The procedure, A, described in ASTM G 65-94 [4], was carried out which corresponds to the conditions summarised in table 4. This is a relatively severe test which will rank materials of medium to extreme abrasion resistance.

The abrasion test results in specimen mass loss. The specimen is thus weighed before and after each test, in order to calculate the mass loss. In general, three specimens were tested for each experimental condition, and the reliability curves were determined assuming a normal distribution.

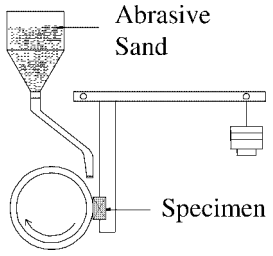

Figure 1. Schematic diagram of the abrasion wear test apparatus.

Table 4
Rubber wheel abrasion test conditions.

Wheel diameter (mm)	224
Wheel width (mm)	13.6
Abrasive	Silica sand
Particle size distribution	80 wt% between 200 and 400 μm
Particle shape	Angular
Abrasive flow (g/min)	300
Rotation speed (rpm)	200
Applied charge (N)	130
Test duration (min)	30
Abrasion linear length (m)	4309

3. Results and discussion

3.1. Microstructure

Figure 2 shows the microstructure observed on the fractured surface of a HVOF spray-coating with 70% of WC + Co. The microstructure was characterised by an overlapping of the WC + Co and the nickel alloy particles. The WC+Co agglomerates are indicated by A in the micrograph of figure 2(b), which corresponds to a mix mode observation, 50% secondary electron detector + 50% backscattered electron detector. WC + Co grains exhibit a lamellar geometry, roughly parallel to the substrate surface, as can be observed in figure 2(b).

Powder flame spraying leads to a microstructure characterised by more equiaxial WC + Co grains with a homogeneous dimension and a more or less regular distribution in the metallic matrix, figure 3. The WC + Co grains are indicated by A in the micrograph shown in figure 3(b).

Remelting the coatings obtained by PFS has a dispersion effect on the WC + Co grains, leading to a more compact microstructure characterised by a very thin dispersion of the WC carbides (indicated by A) in a metallic matrix, as can be seen in figure 4.

The differences observed agree well with the microstructure typical of each process. In the HVOF spraying, the particles undergo moderate heating and impinge on the substrate at supersonic speeds, leading to low porosity and high density coatings with a lamellar structure. Coatings deposited by the PFS technique presented a structure caused by the drops' superposition; that is, a more equiaxial aspect compared with the coatings obtained by HVOF. The higher porosity values found for PFS coatings are due to the low-speed particle spraying.

The remelting of the PFS coating rebuilds the metallographic structure, improving adherence between the matrix and the hard phases. The resulting microstructure is characterised by dispersed small carbides in the metallic matrix, because of the heating applied to the coating to remelt it. The high temperatures allow some cobalt melting. As the WC + Co powders are WC clusters agglomerated by Co, when the cobalt melts it allows the small WC particles to disperse in the matrix, explaining the observed microstructure.

Depending on the spraying techniques used and whether the coatings are remelted or not, several types of microstructures are mentioned in the literature [5–7]. Schwetzke et al. [7] and Barbezat et al. [8] also found that different types of microstructure can be obtained by varying the powder production processes.

3.2. Adhesion

The adhesion of the coatings to the substrate was evaluated by means of pull-testing glued specimens, as mentioned before. Table 3 shows the values of the separation tension obtained for each coating. The values given correspond to

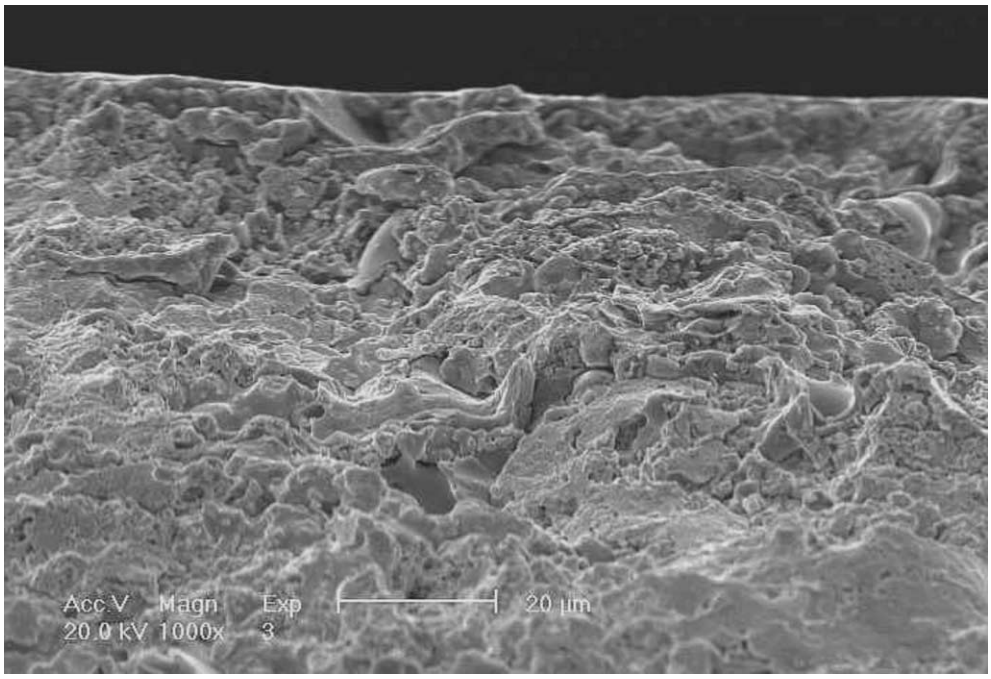

(a)

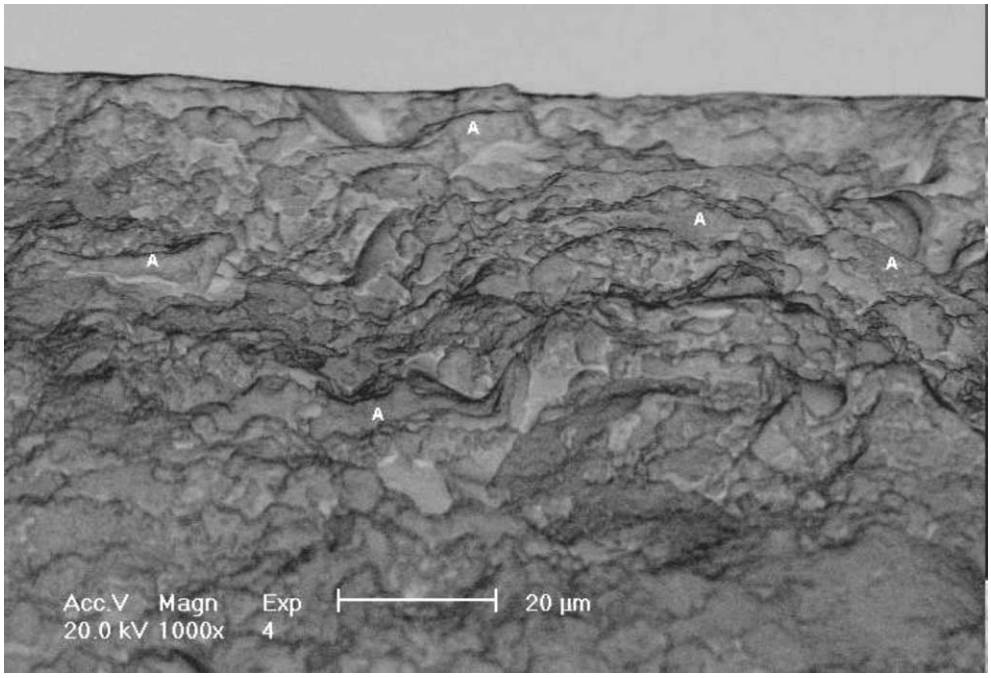

(b)

Figure 2. Microstructures of high-velocity oxy-fuel spraying coating (70% WC + Co), observed by scanning electron microscope on a transversal fractured surface. (a) Secondary electron (SE) observation. (b) Mix mode observation, 50% SE + 50% backscattered electron detector (BS). WC + Co particles are indicated by A.

the average of the three tests. Observation of the specimens' breaking surfaces confirmed that in all cases the separation took place at the interface between the coating and the glue. The coatings cohesion and adhesion is thus higher than the separation tension.

For any of the coatings studied, an increase in the WC + Co content always led to a rise in the adhesive/cohesive tension. Li et al. [9] also reported that an increase in the tungsten carbide phase results in increased adhesion. Higher values of adhesion/cohesion tension were obtained for the HVOF sprayed specimen, table 3. No metallic alloy adhesion layer was applied to the HVOF coatings, in contrast to those sprayed by PFS. The fact that there is WC + Co in the first layers may give higher values for adhesion; however, the HVOF technique by itself already leads to higher adhesion values.

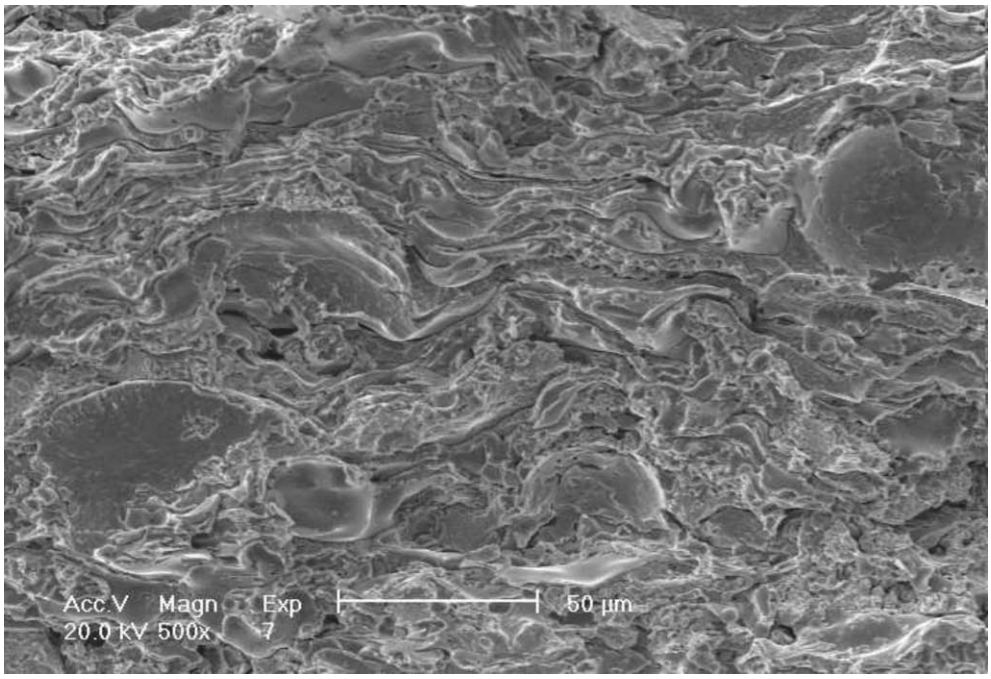

(a)

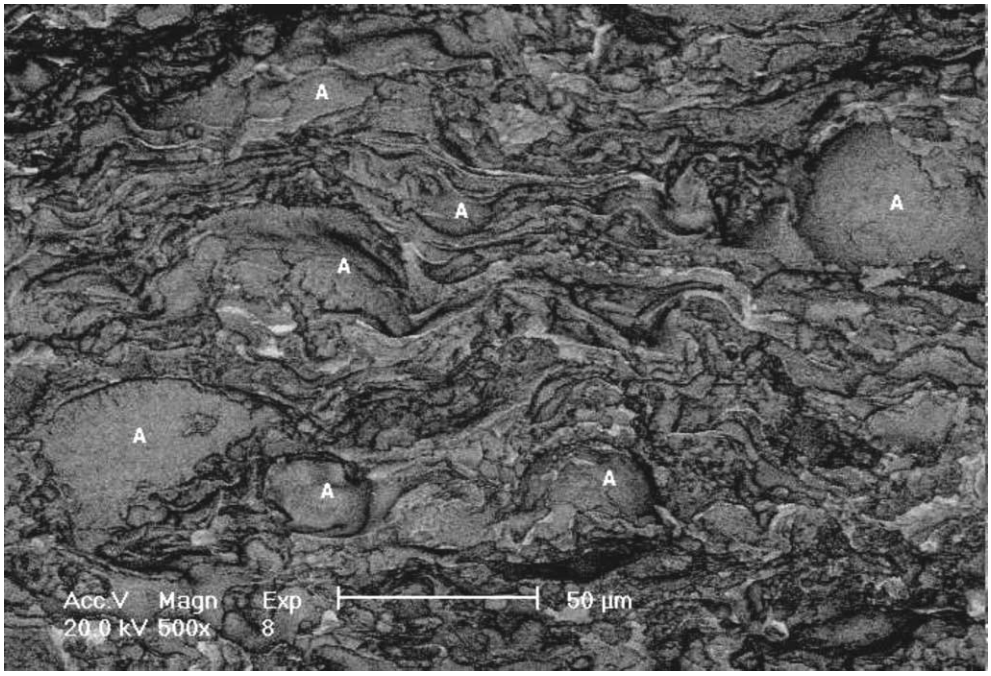

(b)

Figure 3. Microstructures of powder flame spraying coating (70% WC + Co), observed by scanning electron microscope on a transversal fractured surface. (a) Secondary electron (SE) detector. (b) Mix, 50% SE + 50% BS. WC + Co particles are indicated by A.

Concerning the coatings sprayed by PFS, higher adhesion values were found for the sprayed and remelted cases. This may be due to the sort of microstructure obtained with this kind of coating. On remelting, the binder of the WC + Co grains suffered a melting process, also involving the adhesion layer, leading to higher values of adhesion/cohesion tension. The 30% (wt%) WC + Co coating runs contrary to the general tendency of values. In this case, since the quantity of WC + Co is still relatively small, it may be that the remelting has not penetrated the adhesion layer, thus causing the difference observed for the adhesion tension values.

Besides the effects already mentioned, as in general the fracture takes place at the interface between the glue and the coating, the surface texture can play an important role in adhesion. The separation tension may thus depend on the sur-

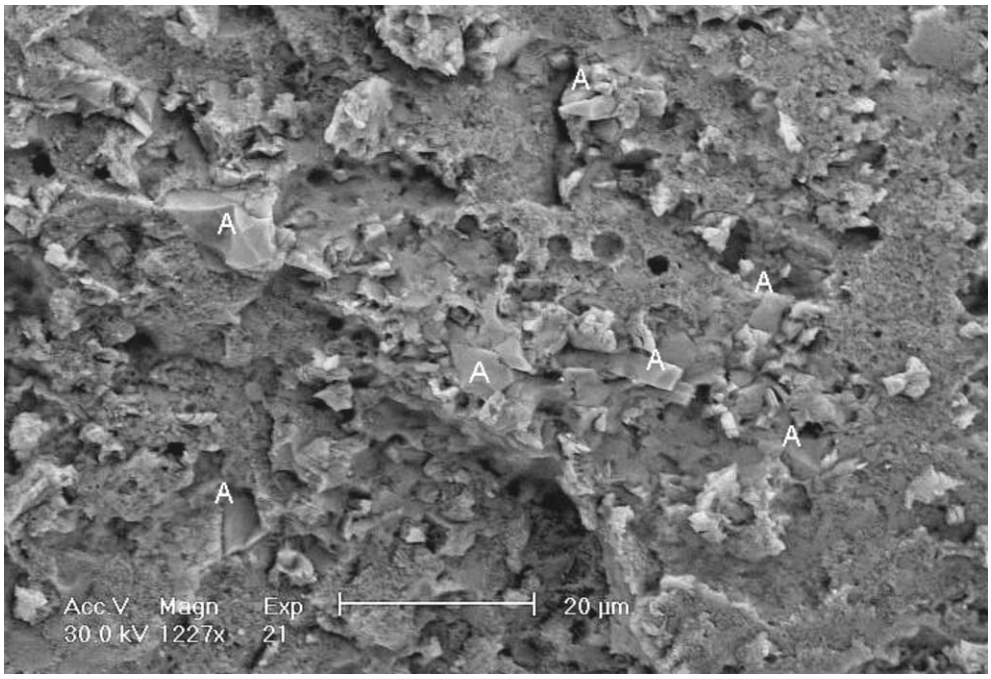

Figure 4. Microstructures of remelted powder flame spraying coating (70% WC+Co), observed by scanning electron microscope on a transversal fractured surface. WC particles are indicated by A.

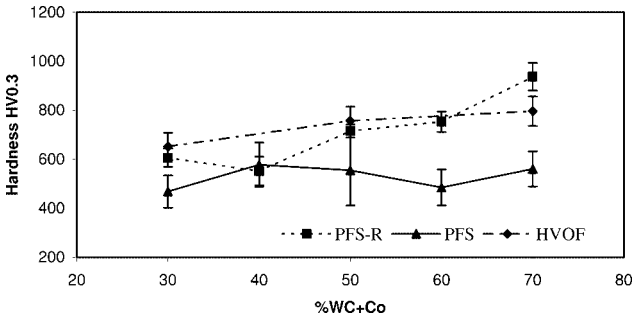

Figure 5. Effect of WC + Co content on coating hardness. Average values and confidence intervals for 95%. HVOF – high-velocity oxy-fuel spraying, PFS – powder flame spraying and PFS-R – powder flame spraying with remelting.

face morphology, which is influenced by the spraying technique used.

3.3. Microhardness

Figure 5 compares the effect of WC + Co content on hardness, for all the techniques used. The highest value of the hardness was obtained for the remelted powder-flame-sprayed coating with the highest WC + Co content. Nevertheless, for the remaining compositions, the higher values were given by the HVOF technique.

While HVOF and the remelted PFS lead to coatings with hardness values that grow as the content of the hard alloy increases, for the as-deposited PFS coatings the hardness values seem to be virtually constant for all the tested compositions. The PFS coatings also exhibit a greater scatter in their microhardness values.

The variation in the hardness of the HVOF and remelted PFS coatings corresponds to what was expected, that is, hardness increasing with increasing hard-phase content. On the as-deposited PFS coating this effect on the hardness is probably eliminated by the increase in porosity.

3.4. Porosity

Analysis of table 3 clearly shows that the HVOF is the process that gives lower porosity coatings. These results are possibly due to the supersonic speeds characteristic of this technique, and to the melting behaviour exhibited by the particles. The particles, partially melted, form an almost porosity-free coating when they reach the substrate at high velocity. The WC + Co content variation does not produce any significant change on the porosity values of the coatings deposited by HVOF.

When the percentage of WC + Co present in the coating was lower than 50% (wt%), the remelting of the PFS coatings led to lower porosity values than the as-sprayed ones; however, for higher WC + Co content the difference in the porosity values is insignificant. In general, a denser microstructure can be expected from remelting because both the matrix and the cobalt melt. For higher WC + Co content, however, the hard phase, which does not melt, remains in the matrix in higher quantities, allowing the formation of small interior hollows that are not filled by the melted material. In addition, during the remelting process, some gases resulting from this operation are retained inside the matrix, because the high content of the hard phase impedes their liberation.

3.5. Phase analysis by X-ray diffraction

In thermal spraying, the degree of phase transformation depends on the thermal energy added to the particles in each spraying process, on the flame temperature and on the particles flying time.

During the thermal spraying of cermets, several carbides are formed, resulting from the oxidation of the sprayed material in the flame and from the occurrence of thermally activated reactions between the WC, the Co and the nickel alloy [10,11].

The main crystalline phases identified in the coatings can be found in table 3.

The HVOF spraying process, with its lower flame temperature and higher particle speed, induces fewer phase transformations in the materials compared with powder flame spraying, with and without remelting. The coatings obtained by HVOF did not undergo significant phase transformations. This is due to the supersonic speeds of the sprayed particles, which expose the particles to a less oxidizing environment, and to the fact that they are exposed to moderate heating. These factors result in coatings with high retention of WC in the matrix.

Mäntylä et al. [10] also observed, for WC + Co coatings, that the high-velocity techniques lead to a higher WC phase content.

3.6. Abrasive wear

Only a small number of abrasion tests were carried out, usually giving three results for each experimental condition. Therefore, in order to obtain more significant results for the standard deviation and for the average, in the analysis of these results, the wear mass-loss values obtained for each WC + Co content have been normalised to give only one population of results for each coating technique. For each coating technique, therefore, the analysis procedure involves the following stages:

(1) with the results of the wear mass-loss M_{ij} for each WC + Co content, where i is associated with one value of WC+Co content and j is the order of the variable (so the range of j is the number of tests done to the specific experimental condition), calculation of the average M_{i0};

(2) normalisation of the test results relative to the average calculated value, M_{i0}, using the expression $X_{ij} = M_{ij}/M_{i0}$;

(3) repeating points 1 and 2 for all the values of WC + Co content (i values);

(4) with the population corresponding to the all-normalised values for each technique (X_{ij} values), determination of the average X_0 and the standard deviation σ;

(5) for each WC + Co content determination of the average m_{i0} and the standard deviation σ_i using the expressions

$$m_{i0} = X_0 M_{i0},$$
$$\sigma_i = \sigma M_{i0};$$

(6) for each WC + Co content, using the m_{i0} and σ_{I} values and the normal law calculation of the value of the wear volume corresponding to the desired reliability.

Figure 6 shows the plotted maximum wear curves, for all of the spraying techniques studied, with 80% reliability, so there is a probability of 80% to obtain wear values lower than the plotted curves. In the same figures the individual symbols represent the experimental results. The remelting process has greatly improved the coatings' abrasion resistance. Wang et al. [2] found a similar effect for plasma-sprayed coatings. As can be observed in figure 6, the remelted coatings yielded the best results for all contents of WC + Co. This improved performance is mainly the result of the changes in microstructure and hardness. In effect, the fusion of the coatings after spraying

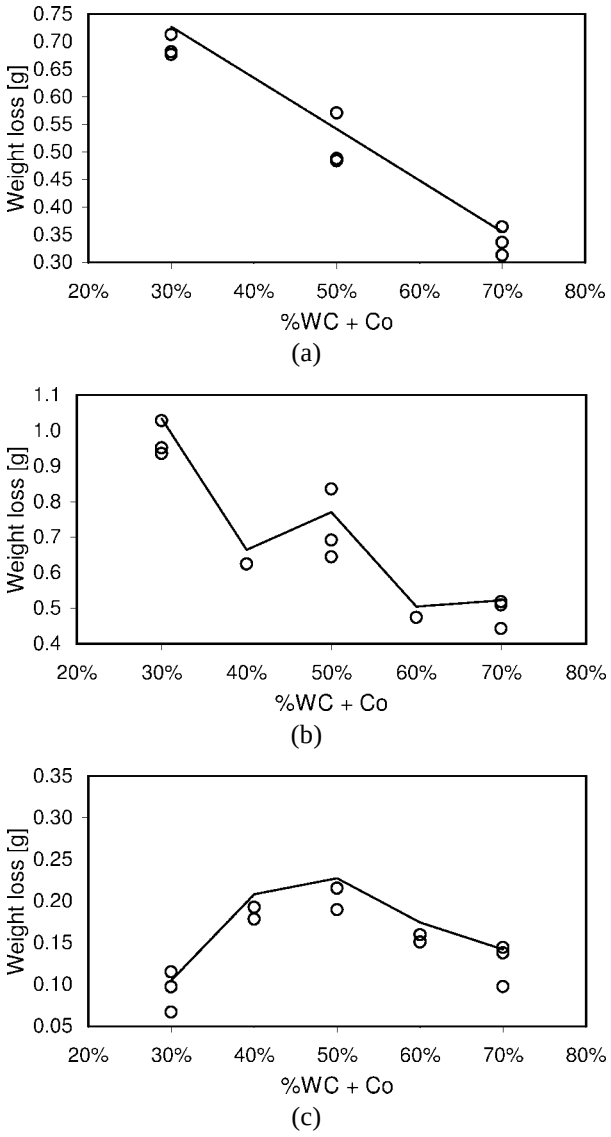

Figure 6. Effect of deposition technique and hard phase content on abrasive wear (reliability = 80%). (a) HVOF – high-velocity oxy-fuel spraying, (b) PFS – powder flame spraying and (c) PFS-R – powder flame spraying with remelting.

causes a thin carbide dispersion in the matrix and also improves the adhesion between the matrix and hard phases. Mäntylä et al. [10] conclude that the higher abrasion resistance on rubber-wheel tests of WC + Co plasma and detonation gun coatings was also obtained for the coatings which had the most uniform microstructure and the finest carbide distribution. Seen et al. [12] have also verified that the reduction of carbide dimensions leads to a significant increase in abrasion resistance for sintered WC + Co. In the present study, the remelted PFS coatings show a behaviour quite different to the other coatings. In fact, for these coatings, the better abrasion resistance has been achieved for the lowest WC + Co content and a maximum wear mass loss occurs for 50% of WC + Co.

The HVOF coatings reveal better abrasion resistance, if compared with those sprayed by PFS. The coatings produced by HVOF reveal the existence of a high level of WC carbide retention, and they also have the highest values of hardness and the lowest of porosity. A combination of all these factors results in a lower mass loss through abrasion for HVOF coatings when compared with the coatings sprayed by PFS.

For the HVOF coatings, an increase in the tungsten carbide percentage results in less wear. Föhl et al. [13] have also concluded that there is an increase in abrasion resistance of their plasma-sprayed coatings, when WC is incorporated at varied percentages, from 0 to 50%. Likewise, Senn et al. [12] attributed a rise in abrasion resistance of sintered WC + Co to a decrease in the metallic phase.

As with the HVOF, the as-deposited PFS coatings seem to have a tendency to increased abrasion resistance with a growth in the hard-phase content.

3.7. Wear model

Axén et al. [14] derived a model for appraising the abrasion resistance of multiphase materials which depends on the wear resistance demonstrated by the materials' constituents when tested separately. This model uses two equations that explain the limits, superior EW (equal wear) and inferior EP (equal pressure) of the multiphase material's abrasion resistance. These limits correspond to two distinct situations of load. The superior limit corresponds to an equal wear case and the load is supported by the matrix, while for the inferior limit, that corresponds to an equal pressure, the load is supported by the hard phase particles.

Since in the abrasion "rubber-wheel" test the abrasion grains are supported by a surface of low hardness (rubber), it might be expected that the results would be in accordance with the model of equal pressure (EP). However, as shown in figure 7, the wear resistance evolution of the sprayed coatings, whether by HVOF or by PFS, is linear with the volumetric percentage of the hard phase, and thus closer to what this model predicts for the equal wear (EW) situations.

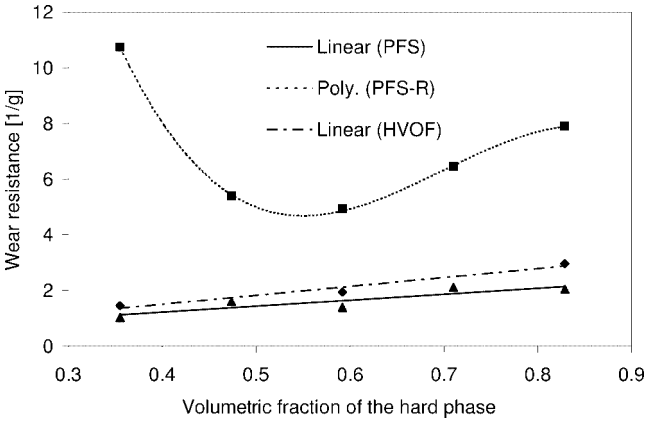

Figure 7. Coating abrasion resistance versus volumetric fraction of the hard phase. HVOF – high-velocity oxy-fuel spraying, PFS – powder flame spraying and PFS-R – powder flame spraying with remelting.

It is not possible to fit the curve obtained for the behaviour of the remelted coatings into one of the two situations of the Axén model. In this case, owing to the remelting, the WC carbide dispersion in the matrix has given rise to a structure with a very thin WC dispersion, and therefore with a very similar behaviour to that of conventional bulk materials, like melted iron or steel. In addition, the probable decrease in the fracture toughness, as the WC + Co content increases, may have caused the lack of linearity of the curve obtained, resulting in changes in wear mechanism.

As the experimental results obtained for both the PFS and HVOF coatings show a reasonable linear correlation, it is possible to determine equations that may be used to predict the behaviour of cermet coatings whose WC + Co content is intermediate to those used in this study.

For the HVOF coatings, therefore, the following equation has been derived:

$$\Omega = 3.20\nu + 0.22.$$

The as-deposited powder flame sprayed coatings fit well with the equation

$$\Omega = 2.13\nu + 0.37.$$

Here Ω is abrasion wear resistance (1/g) and ν is the volumetric fraction of the hard phase.

3.8. Wear mechanisms

Observation of the wear surfaces revealed that the wear scars of the coatings obtained by HVOF, figure 8, and by powder flame spraying without remelting, figure 9, reveal a carbide distribution protruding from the surface. Besides this, we can observe much larger WC + Co grains distribution for the HVOF spraying than for the other case, figure 8(a).

The remelting of the coatings gives rise to very flat abrasion surfaces, with fine carbides highly dispersed in the matrix, figure 10.

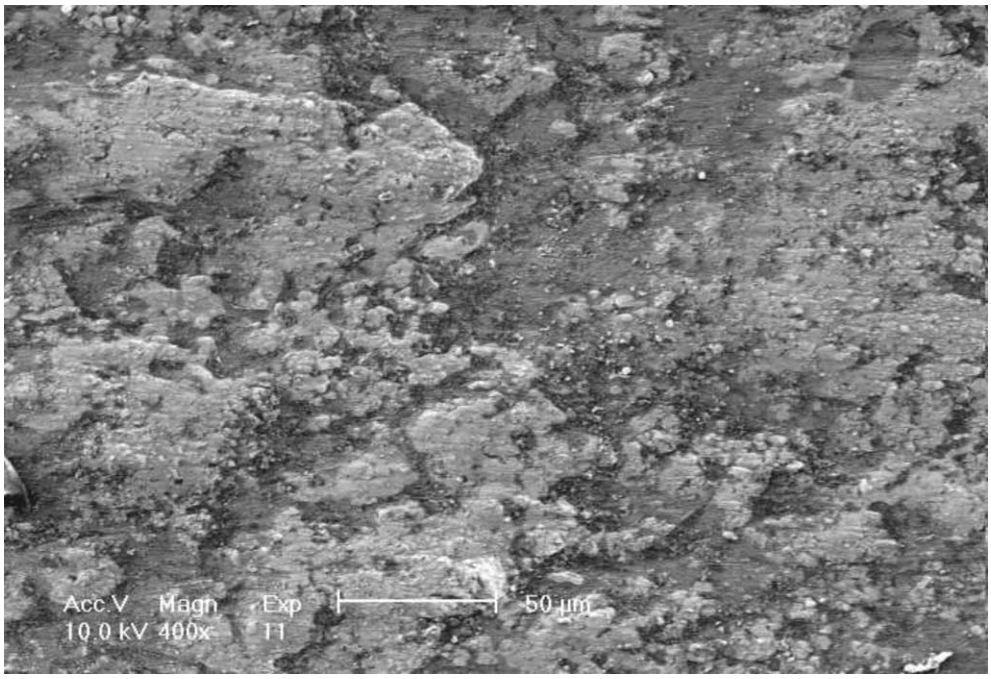

(a)

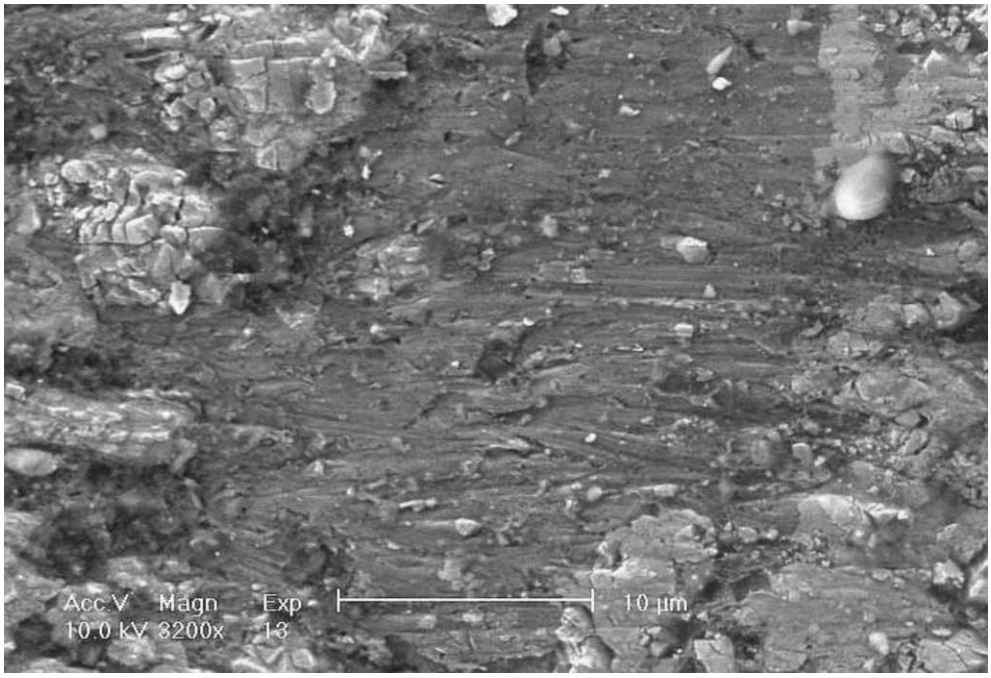

(b)

Figure 8. Worn surface morphology of high-velocity oxy-fuel sprayed coating (70% WC + Co), observed at different magnifications.

Concerning the HVOF and the as-deposited PFS coatings, the wear mechanism observed on the surface consists of two distinct phases:

(1) matrix removal by two-body abrasion;

(2) fragmentation and separation of the carbide grains.

This phenomenon has already been observed and described by other authors [13,15–18]. Thus, in a first stage, these is preferential wear, and matrix cutting occurs through a process of two-body abrasion, figures 8(b) and 11. In this stage, the abrasive penetrates the ductile matrix, creating wear valleys. Matrix ploughing also occurs, because the abrasive particles apply cyclical tangential and normal forces to the carbide grains.

The continuous removal of the metallic matrix gives a surface from which the carbide grains stand out relative to the surface. In figure 9(a) it can be clearly seen that the carbide grains are standing out from the matrix.

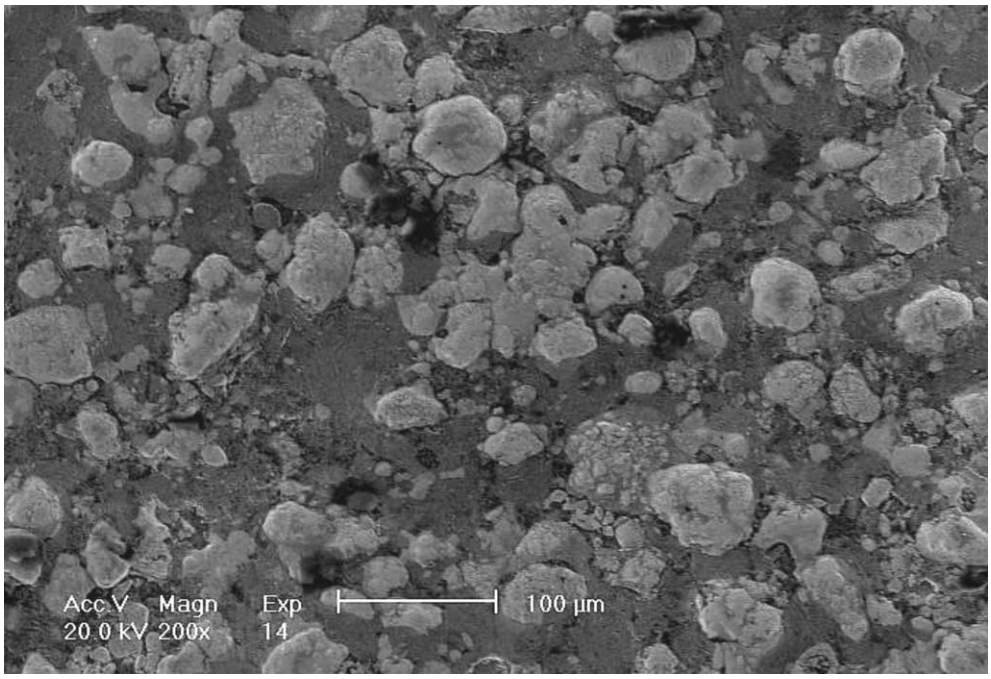

(a)

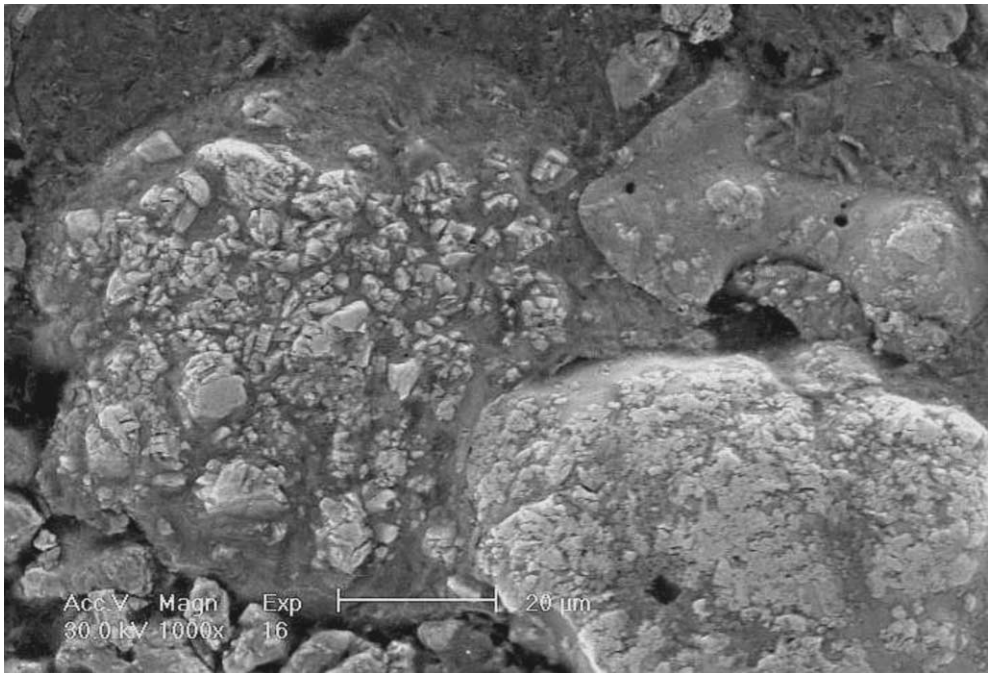

(b)

Figure 9. Worn surface morphology of powder flame sprayed coating (70% WC + Co), observed at different magnifications.

During a second stage, due to the continuous matrix removal, which significantly reduces the carbides' supporting capacity, a point is reached at which the WC + Co grains remain salient and consequently are submitted to a higher pressure. As the matrix is worn, the WC + Co are gradually dispersed, owing to deformation of their cobalt binder, and some WC small grains are removed by the abrasive particles. In figures 9(b) and 11 the desegregation of some WC + Co particles can be seen. When this state is reached, the carbide particles lose their support and they become detached.

Coating remelting leads to carbide cluster dispersion, to form a structure characterised by thin carbide dispersion in a matrix with a sufficient hardness/toughness relation, figure 10. This structure exhibits an abrasion resistance that is altogether superior to that obtained with the rest of the coatings.

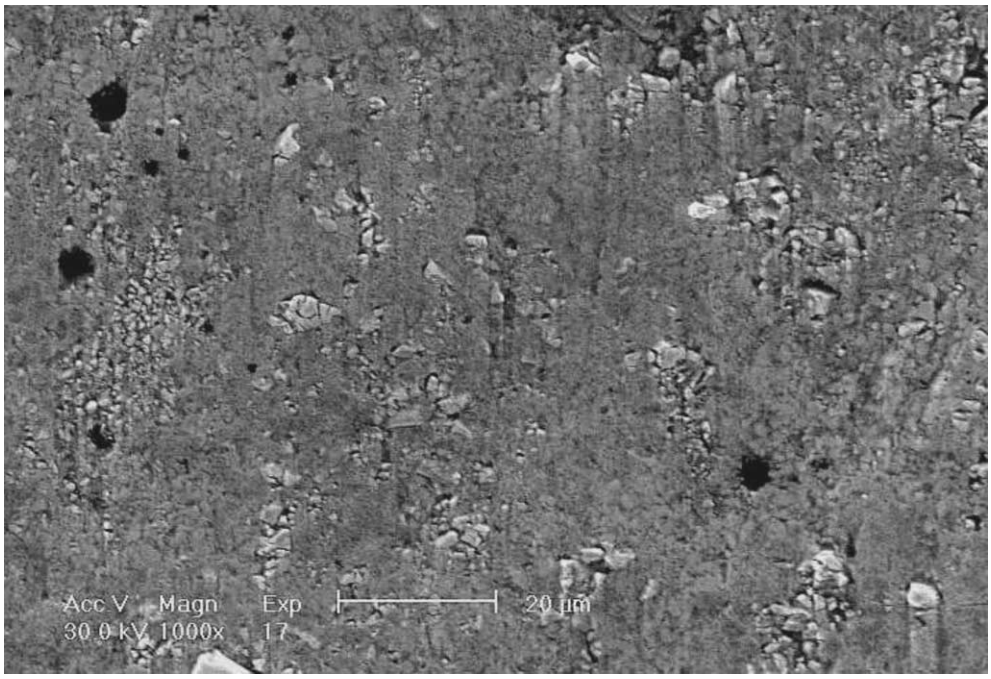

Figure 10. Worn surface morphology of remelted powder flame sprayed coating (70% WC + Co).

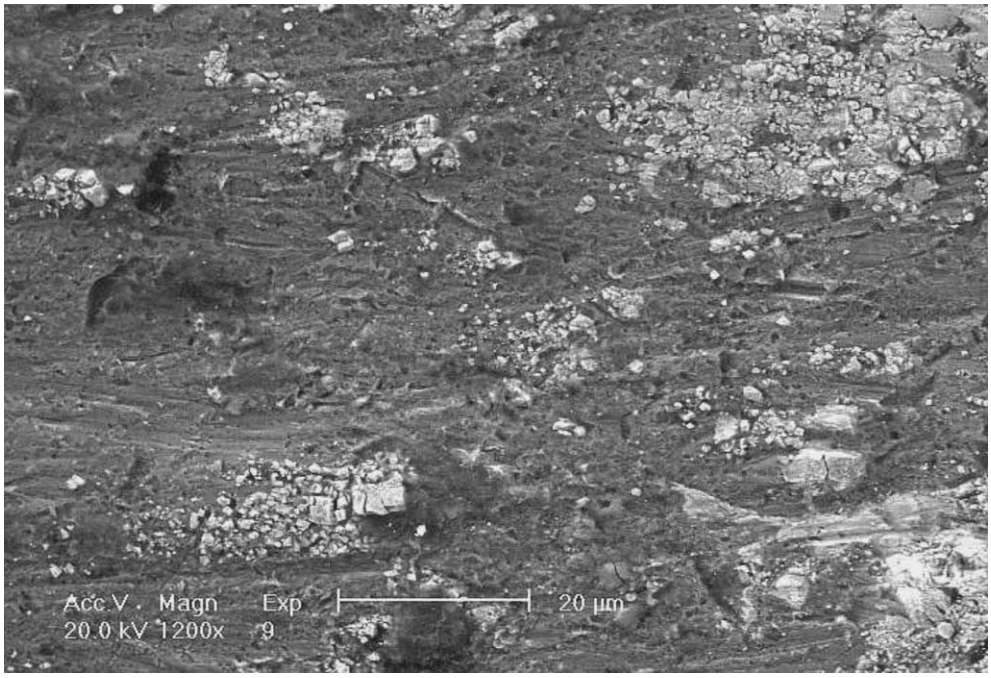

Figure 11. Details of the worn surface of powder flame sprayed coating (70% WC + Co).

4. Conclusions

This comparative study of the properties of coatings with WC + Co in a metallic matrix obtained by different spraying techniques has made it possible to conclude that:

- The increase of the fraction corresponding to the WC + Co hard phase produces an increase in substrate adhesion for all the spraying techniques used.
- The HVOF deposited coatings have better adhesion than those sprayed by powder flame spraying, with or without remelting after spraying.
- For the coatings produced by powder flame spraying, the remelting after spraying led to increased adhesion to the substrate, especially in the coatings with a larger WC + Co percentage.
- The remelting undertaken with the powder flame sprayed coatings produced quite significant hardness

gains, thereby obtaining the hardest coatings of those tested in this work. The hardness of the remelted coatings increased with increasing WC + Co content.

- The main wear mechanism that occurs in the HVOF and powder flame spraying coatings was identified by the development of two stages:
  - matrix removal by abrasion, leaving projecting WC + Co grains;
  - dispersion of the WC + Co agglomerates and separation of WC grains.
- The experimental results for the abrasion resistance of the as-deposited coated specimens, produced by HVOF and by powder flame spraying, fit well with the Axén model for abrasion resistance of composite materials. Using that model, when the volumetric fraction (ν) of the WC + Co phase ranges from 30 to 70 wt%. the abrasion resistance (Ω) can be calculated by the following equations:

$$\text{HVOF} \qquad \Omega = 3.20\nu + 0.22,$$
$$\text{PCSR} \qquad \Omega = 2.13\nu + 0.37.$$

Acknowledgement

The authors would like to express their thanks to António Gonçalves, Engineer, from the Centro Tecnológico da Cerâmica e do Vidro – Coimbra, for his help in producing the HVOF coatings.

References

[1] G. Barbezat, J.R. Moens and A.R. Nicoll, Sulzer Technical Review 2 (1991) 26.
[2] H. Wang, W. Xia and Y. Jin, Wear 195 (1996) 47.
[3] ASTM C 633-79, Standard Test Method for Adhesion or Cohesive Strength of Flame – Sprayed Coatings.
[4] ASTM G 65-94, Standard Test Method for Measuring Abrasion Using the Dry Sand/Rubber Wheel Apparatus.
[5] G.R. Heath and R.J. Dumola, in: *Proc. 15th Int. Thermal Spray Conference*, Nice, 1998, p. 1495.
[6] G. Barbezat, A.R. Nicoll and A. Sickinger, Wear 162–164 (1993) 529.
[7] R. Schwetzke and H. Kreye, in: *Proc. 15th Int. Thermal Spray Conference*, Nice, 1998, p. 187.
[8] G. Barbezat, E. Müller and B. Walser, Sulzer Technical Review 4 (1988) 4.
[9] C.J. Li and H. Li, in: *Proc. 15th Int. Thermal Spray Conference*, Nice, 1998, p. 728.
[10] T.A. Mäntylä, K.J. Niemi and P.M.J. Vuoristo, in: *Proc. 2nd Plasma-Technik Symposium*, Luzern, 1991, p. 287.
[11] M.E. Vinayo, F. Kassabji, J. Guionnet and P. Fauchais, J. Vac. Sci. Technol. A 3 (1986) 2483.
[12] R.H. Senn, N.E. Jee, D.J. Treacy and M.K. Keshavan, in: *Proc. Conf. of Corrosion–Erosion Wear of Materials at Elevated Temperatures*, Berkeley, 1986, p. 299.
[13] J. Föhl, T. Weissenberg and J. Wiedemeyer, Wear 130 (1989) 275.
[14] N. Axén and S. Jacobson, Wear 174 (1994) 187.
[15] D. Scott, ed., *Treatise on Materials Science and Technology* (Academic Press, London, 1979).
[16] I.M. Hutchings, *Tribology – Friction and Wear of Engineering Materials*, Cambridge, 1992.
[17] J. Larsen-Basse and E.T. Koyanagi, Trans. ASME 101 (1979) 208.
[18] S.F. Scieszka and K. Filipowicz, Wear 216 (1998) 202.